

# Non-Symmetrized Hyperspherical Harmonics Method for Non-Equal Mass Three-Body Systems

A. Nannini<sup>1,2</sup> and L.E. Marcucci<sup>1,2</sup>

<sup>1</sup>*Dipartimento di Fisica “Enrico Fermi”, Università di Pisa, Largo Bruno Pontecorvo 3 - I-56127 Pisa, Italy*

<sup>2</sup>*Istituto Nazionale di Fisica Nucleare, Sezione di Pisa,  
Largo Bruno Pontecorvo 3 - I-56127 Pisa, Italy*

The non-symmetrized hyperspherical harmonics method for a three-body system, composed by two particles having equal masses, but different from the mass of the third particle, is reviewed and applied to the  ${}^3\text{H}$ ,  ${}^3\text{He}$  nuclei and  ${}^3_\Lambda\text{H}$  hyper-nucleus, seen respectively as  $nnp$ ,  $ppn$  and  $NN\Lambda$  three-body systems. The convergence of the method is first tested in order to estimate its accuracy. Then, the difference of binding energy between  ${}^3\text{H}$  and  ${}^3\text{He}$  due to the difference of the proton and the neutron masses is studied using several central spin-independent and spin-dependent potentials. Finally, the  ${}^3_\Lambda\text{H}$  hypernucleus binding energy is calculated using different  $NN$  and  $\Lambda N$  potential models. The results have been compared with those present in the literature, finding a very nice agreement.

## I. INTRODUCTION

The hyperspherical harmonics (HH) method has been widely applied in the study of the bound states of few-body systems, starting from  $A = 3$  nuclei [1, 2]. Usually, the use of the HH basis is preceded by a symmetrization procedure that takes into account the fact that protons and neutrons are fermions, and the wave function has to be antisymmetric under exchange of any pair of these particles. For instance, for  $A = 3$ , antisymmetry is guaranteed by writing the wave function as

$$\Psi = \sum_p \Psi_p, \quad (1)$$

$p = 1, 2, 3$  corresponding to the three different particle permutations [1]. However, it was shown in Refs. [3–7] that this preliminary step is in fact not strictly necessary, since, after the diagonalization of the Hamiltonian, the eigenvectors turn out to have a well-defined symmetry under particle permutation. In this second version, the method is known as non-symmetrized hyperspherical harmonics (NSHH) method. As we will also show below, the prize to pay for the non-antisymmetrization is that a quite larger number of the expansion elements are necessary with respect to the “standard” HH method. However, the NSHH method has the advantage to reduce the computational effort due to the symmetrization procedure, and, moreover, the same expansion can be easily re-arranged for systems of different particles with different masses. In fact, the steps to be done within the NSHH method from the case of equal-mass to the case of non-equal mass particles are quite straightforward and will be illustrated below. In this work, we apply the NSHH method to study the  ${}^3\text{H}$ ,  ${}^3\text{He}$  and  ${}^3_\Lambda\text{H}$  systems, seen as  $nnp$ ,  $ppn$ ,  $NN\Lambda$  respectively (we used the standard notation of  $N$  for nucleon and  $Y$  for hyperon). In order to test our method, we study the first two systems listed above with five different potential models, and the hypernucleus with three potential models. We start with simple central spin-independent  $NN$  and  $YN$  interactions, and then we move to central spin-dependent potentials. To be noticed that none of the interactions considered is realistic. Furthermore, we do not include three-body forces. Therefore, the comparison of our results with the experimental data is meaningless. However, the considered interactions are useful to test step by step our method and to compare with results obtained in the literature.

The paper is organized as follows: in Section II we describe the NSHH method, in Section III we discuss the results obtained for the considered nuclear systems. Some concluding remarks and an outlook are presented in Section IV.

## II. THEORETICAL FORMALISM

We briefly review the formalism of the present calculation. We start by introducing the Jacobi coordinates for a system of  $A = 3$  particles, with mass  $m_i$ , position  $\mathbf{r}_i$ , and momentum  $\mathbf{p}_i$ . By defining  $\mathbf{x}_i = \sqrt{m_i} \mathbf{r}_i$  [8], they are taken as a linear combination of  $\mathbf{x}_i$ , i.e.

$$\mathbf{y}_i = \sum_{j=1}^A c_{ij} \mathbf{x}_j, \quad (2)$$

where the coefficients  $c_{ij}$  need to satisfy the following conditions [8]

$$\sum_{i=1}^3 c_{ji}c_{ji} = \frac{1}{M} \quad (j = 1, 2) , \quad (3)$$

$$\sum_{i=1}^3 c_{ji}c_{ki} = 0 \quad (j \neq k = 1, 2) . \quad (4)$$

Here  $M$  is a reference mass. The advantage of using Eqs. (2)–(4) is that the kinetic energy operator can be cast in the form

$$T = -\frac{\hbar^2}{2m_{tot}}\nabla_{\mathbf{y}_3}^2 - \frac{\hbar^2}{2M}(\nabla_{\mathbf{y}_1}^2 + \nabla_{\mathbf{y}_2}^2) , \quad (5)$$

where  $\mathbf{y}_3$  is the center-of-mass coordinate. For a three-body system, there are three possible permutations of the particles. Therefore, the Jacobi coordinates depend on this permutations. For  $p = 3$ , i.e.  $i, j, k = 1, 2, 3$ , the Jacobi coordinates are explicitly given by

$$\begin{aligned} \mathbf{y}_2^{(3)} &= -\sqrt{\frac{m_2}{M(m_1+m_2)}}\mathbf{x}_1 + \sqrt{\frac{m_1}{M(m_1+m_2)}}\mathbf{x}_2 , \\ \mathbf{y}_1^{(3)} &= -\sqrt{\frac{m_1m_3}{Mm_{tot}(m_1+m_2)}}\mathbf{x}_1 - \sqrt{\frac{m_2m_3}{Mm_{tot}(m_1+m_2)}}\mathbf{x}_2 + \sqrt{\frac{m_1+m_2}{Mm_{tot}}}\mathbf{x}_3 . \end{aligned} \quad (6)$$

They reduce to the familiar expressions for equal-mass particles when  $m_1 = m_2 = m_3 = M$  (see for instance Ref. [1]). We then introduce the hyperspherical coordinates, by replacing, in a standard way, the moduli of  $\mathbf{y}_{1,2}^{(3)}$  by the hyperradius and one hyperangle, given by

$$\rho^2 = \mathbf{y}_1^{(p)2} + \mathbf{y}_2^{(p)2} , \quad (7)$$

$$\tan \phi^{(p)} = \frac{y_1^{(p)}}{y_2^{(p)}} . \quad (8)$$

To be noticed that the hyperangle  $\phi^{(p)}$  depends on the permutation  $p$ , while the hyperradius  $\rho$  does not. The well-known advantage of using the hyperspherical coordinates is that the Laplace operator can be cast in the form [8]

$$\nabla^2 = \nabla_{\mathbf{y}_1}^2 + \nabla_{\mathbf{y}_2}^2 = \frac{\partial^2}{\partial \rho^2} + \frac{5}{\rho} \frac{\partial}{\partial \rho} + \frac{\Lambda^2(\Omega^{(p)})}{\rho^2} , \quad (9)$$

where  $\Lambda^2(\Omega^{(p)})$  is called the grand-angular momentum operator, and is explicitly written as

$$\Lambda^2(\Omega^{(p)}) = \frac{\partial^2}{\partial \phi^{(p)2}} - \frac{\hat{\ell}_1^2(\hat{\mathbf{y}}_1^{(p)})}{\sin^2 \phi^{(p)}} - \frac{\hat{\ell}_2^2(\hat{\mathbf{y}}_2^{(p)})}{\cos^2 \phi^{(p)}} + 2 \left[ \cot \phi^{(p)} - \tan \phi^{(p)} \right] \frac{\partial}{\partial \phi^{(p)}} . \quad (10)$$

Here  $\hat{\ell}_1^2$  and  $\hat{\ell}_2^2$  are the (ordinary) angular momentum operators associated with the Jacobi vectors  $\mathbf{y}_1^{(p)}$  and  $\mathbf{y}_2^{(p)}$  respectively, and  $\Omega^{(p)} \equiv (\hat{\mathbf{y}}_1^{(p)}, \hat{\mathbf{y}}_2^{(p)}, \phi^{(p)})$ . The HH functions are the eigenfunctions of the grand-angular momentum operator  $\Lambda^2(\Omega^{(p)})$ , with eigenvalue  $-G(G+4)$ , i.e.

$$\Lambda^2(\Omega^{(p)})Y_G(\Omega^{(p)}) = -G(G+4)Y_G(\Omega^{(p)}) . \quad (11)$$

Here the HH function  $Y_G(\Omega^{(p)})$  is defined as

$$\begin{aligned} Y_G(\Omega^{(p)}) &= N_n^{\ell_1, \ell_2} (\cos \phi^{(p)})^{\ell_2} (\sin \phi^{(p)})^{\ell_1} Y_{\ell_1 m_1}(\hat{\mathbf{y}}_1^{(p)}) Y_{\ell_2 m_2}(\hat{\mathbf{y}}_2^{(p)}) \\ &\times P_n^{\ell_1 + \frac{1}{2}, \ell_2 + \frac{1}{2}}(\cos 2\phi^{(p)}) , \end{aligned} \quad (12)$$

with  $N_n^{\ell_1, \ell_2}$  a normalization factor [8] and

$$G = 2n + \ell_1 + \ell_2 , \quad n = 0, 1, \dots , \quad (13)$$

$ch$	$\Lambda$	$\Sigma$	$G^{min}$
1	0	1/2	0
2	1	1/2	2
3	1	3/2	2
4	2	3/2	2

TABLE I: List of the channels for a  $J^\pi = 1/2^+$  system.  $\Lambda$  and  $\Sigma$  are the total orbital angular momentum and the total spin of the nuclei. See text for more details.

is the so-called grand-angular momentum. We remark that the HH functions depend on the considered permutation via  $\Omega^{(p)}$ . It is useful to combine the HH functions in order to assign them a well defined total orbital angular momentum  $\Lambda$ . Using the Clebsch-Gordan coefficients, we introduce the functions  $H_G(\Omega^{(p)})$  as

$$\begin{aligned} H_G(\Omega^{(p)}) &= \sum_{m_1, m_2} Y_G(\Omega^{(p)})(\ell_1 m_1 \ell_2 m_2 | \Lambda \Lambda_z) \\ &\equiv [Y_{\ell_1}(\hat{\mathbf{y}}_1^{(p)}) Y_{\ell_2}(\hat{\mathbf{y}}_2^{(p)})]_{\Lambda, \Lambda_z} P_n^{\ell_1, \ell_2}(\phi^{(p)}) , \end{aligned} \quad (14)$$

where  $[G]$  stands for  $[\ell_1, \ell_2, \Lambda, n]$ , and

$$P_n^{\ell_1, \ell_2}(\phi^{(p)}) = N_n^{\ell_1, \ell_2} (\cos \phi^{(p)})^{\ell_2} (\sin \phi^{(p)})^{\ell_1} P_n^{\ell_1 + \frac{1}{2}, \ell_2 + \frac{1}{2}}(\cos 2\phi^{(p)}) . \quad (15)$$

We now consider our system made of three particles, two with equal masses, different from the mass of the third particle. We choose to fix the two equal mass particles in position 1 and 2, and we set the third particle with different mass as particle 3. Therefore, we will work with the Jacobi and hyperspherical coordinates with fixed permutation  $p = 3$ .

The wave function that describes our system can now be cast in the form

$$\Psi = \sum_{\{G\}} BH_{\{G\}}^J(\Omega^{(3)}) u_{\{G\}}(\rho) , \quad (16)$$

where  $u_{\{G\}}(\rho)$  is a function of only the hyperradius  $\rho$ , and  $BH_{\{G\}}^J(\Omega^{(3)})$  is given by Eq. (14) multiplied by the spin part, i.e.

$$BH_{\{G\}}^J(\Omega^{(3)}) = \sum_{\Lambda_z, \Sigma_z} H_{[G]}(\Omega^{(3)}) \times \left[ \left[ \frac{1}{2} \otimes \frac{1}{2} \right]_{S, s} \otimes \frac{1}{2} \right]_{\Sigma, \Sigma_z} \times (\Lambda \Lambda_z, \Sigma \Sigma_z | J J_z) . \quad (17)$$

Here  $S$  is the spin of the first couple with third component  $s$ ,  $\Sigma$  is the total spin of the system and  $\Sigma_z$  its third component, and  $\{G\}$  now stands for  $\{\ell_1, \ell_2, n, \Lambda, S, \Sigma\}$ . To be noticed that the  $LS$ -coupling scheme is used, so that the total spin of the system is combined, using the Clebsch-Gordan coefficient  $(\Lambda \Lambda_z, \Sigma \Sigma_z | J J_z)$ , with the total orbital angular momentum to give the total spin  $J$ . Furthermore, (i)  $\ell_1, \ell_2$  and  $n$  are taken such that Eq. (13) is satisfied for  $G$  that runs from  $G^{min} = \ell_1 + \ell_2$  to a given  $G^{max}$ , to be chosen in order to reach the desired accuracy, and (ii) we have imposed  $\ell_1 + \ell_2 = \text{even}$ , since the systems under consideration have positive parity. The possible values for  $\Lambda, \Sigma$ , and  $G^{min}$ , which together with  $G^{max}$  identify a channel, are listed in Table I for a system with  $J^\pi = 1/2^+$ . Note that, since we are using central potentials, only the first channel of Table I will be in fact necessary.

In the present work, the hyperradial function is itself expanded on a suitable basis, i.e. a set of generalized Laguerre polynomials [1]. Therefore, we can write

$$u_{\{G\}}(\rho) = \sum_l c_{\{G\}, l} f_l(\rho) , \quad (18)$$

where  $c_{\{G\}, l}$  are unknown coefficients, and

$$f_l(\rho) = \sqrt{\frac{l!}{(l+5)!}} \gamma^3 {}^{(5)}L_l(\gamma\rho) e^{-\frac{\gamma}{2}\rho} . \quad (19)$$

Here  ${}^{(5)}L_l(\gamma\rho)$  are generalized Laguerre polynomials, and the numerical factor in front of them is chosen so that  $f_l(\rho)$  are normalized to unit. Furthermore,  $\gamma$  is a non-linear parameter, whose typical values are in the range  $(2 - 5) \text{ fm}^{-1}$ .

The results have to be stable against  $\gamma$ , as we will show in Section III. With these assumptions, the functions  $f_l(\rho)$  go to zero for  $\rho \rightarrow \infty$ , and constitute an orthonormal basis.

By using Eq. (18), the wave function can now be cast in the form

$$\Psi = \sum_{\{G\}} \sum_{l=1}^{N_{max}} c_{\{G\},l} BH_{\{G\}}^J(\Omega) f_l(\rho) , \quad (20)$$

where we have dropped the superscript (3) in  $\Omega^{(3)}$  to simplify the notation, and we have indicated with  $N_{max}$  the maximum number of Laguerre polynomials in Eq. (18).

In an even more compact notation, we can write

$$\Psi = \sum_{\xi} c_{\xi} \Psi_{\xi} , \quad (21)$$

where  $\Psi_{\xi}$  is a complete set of states, and  $\xi$  is the index that labels all the quantum numbers defining the basis elements. The expansion coefficients  $c_{\xi}$  can be determined using the Rayleigh-Ritz variational principle [1], which states that

$$\langle \delta_c \Psi | H - E | \Psi \rangle = 0 , \quad (22)$$

where  $\delta_c \Psi$  denotes the variation of the wave function with respect to the coefficients  $c_{\xi}$ . By doing the differentiation, the problem is then reduced to a generalized eigenvalue-eigenvector problem of the form

$$\sum_{\xi'} \langle \Psi_{\xi} | H - E | \Psi_{\xi'} \rangle c_{\xi'} = 0 , \quad (23)$$

that is solved using the Lanczos diagonalization algorithm [9]. The use of the Lanczos algorithm is dictated by the large size ( $\sim 50000 \times 50000$ ) of the involved matrices (see below).

All the computational problem is now shifted in having to calculate the norm, kinetic energy and potential energy matrix elements. One of the advantage of using a fixed permutation is that the norm and kinetic energy matrix elements are or analytical, or involve just a one-dimensional integration. In fact, they are written as

$$N_{\{G'\},k;\{G\},l} \equiv \langle \Psi_{\xi'} | \Psi_{\xi} \rangle = J \delta_{\xi,\xi'} , \quad (24)$$

$$\begin{aligned} T_{\{G'\},k;\{G\},l} &\equiv \langle \Psi_{\xi'} | T | \Psi_{\xi} \rangle = -\frac{\hbar^2}{2M} J \delta_{\{G'\},\{G\}} \int d\rho \rho^5 f_k(\rho) \\ &\times \left[ -G(G+4) \frac{f_l(\rho)}{\rho^2} + 5 \frac{f_l'(\rho)}{\rho} + f_l''(\rho) \right] , \end{aligned} \quad (25)$$

where  $J$  is the total Jacobian of the transformation, given by

$$J = \left( M \sqrt{\frac{m_{tot}}{m_1 m_2 m_3}} \right)^3 , \quad (26)$$

and  $f_l'(\rho)$  and  $f_l''(\rho)$  are, respectively, the first and the second derivatives of the functions  $f_l(\rho)$  defined in Eq. (19).

The potential matrix elements in Eq. (23) can be written as

$$V_{\{G'\},k;\{G\},l} \equiv \langle \Psi_{\xi'} | V_{12} + V_{23} + V_{13} | \Psi_{\xi} \rangle , \quad (27)$$

with  $V_{ij}$  indicating the two-body interaction between particle  $i$  and particle  $j$ . Note that in the present work we do not consider three-body forces. Since it is easier to evaluate the matrix elements of  $V_{ij}$  when the Jacobi coordinate  $\mathbf{y}_2$  is proportional to  $\mathbf{r}_i - \mathbf{r}_j$ , we proceed as follows. We make use of the fact that the hyperradius is permutation-independent, and we use the fact that the HH function written in terms of  $\Omega^{(p)}$  can be expressed as function of the HH written using  $\Omega^{(p')}$ , with  $p' \neq p$ . Basically it can be shown that [1]

$$H_{[G]}(\Omega^{(p)}) = \sum_{[G']} a_{[G],[G']}^{(p \rightarrow p'),G,\Lambda} H_{[G']}(\Omega^{(p')}) , \quad (28)$$

where the grandangular momentum  $G$  and the total angular momentum  $\Lambda$  remain constant, i.e.  $G = G'$  and  $\Lambda = \Lambda'$ , but we have  $[G] \neq [G']$ , since all possible combinations of  $\ell_1, \ell_2, n$  are allowed. The spin-part written in terms of

permutation  $p$  can be easily expressed in terms of permutation  $p'$  via the standard  $6j$  Wigner coefficients [10]. The transformation coefficients  $a_{[G],[G']}^{(p \rightarrow p'),G}$  can be calculated, for  $A = 3$ , through the Raynal-Revai recurrence relations [11]. Alternately we can use the orthonormality of the HH basis [1], i.e.

$$a_{[G],[G']}^{(p \rightarrow p'),G,\Lambda} = \int d\Omega^{(p')} [H_{[G']}(\Omega^{(p')})]^\dagger H_{[G]}(\Omega^{(p)}) . \quad (29)$$

Their explicit expression can be found for instance in Ref. [1] as is reported in the Appendix for completeness. The final expression for the potential matrix elements is given by

$$\begin{aligned} \langle \Psi_{\xi'} | V_{12} + V_{23} + V_{13} | \Psi_{\xi} \rangle = & J \int d\rho \rho^5 f_k(\rho) f_l(\rho) \\ & \times \left\{ \int d\Omega^{(3)} B H_{\xi'}^\dagger(\Omega^{(3)}) V_{12} B H_{\xi}(\Omega^{(3)}) \right. \\ & + \sum_{\xi''} \sum_{\xi'''} \left[ a_{\xi' \rightarrow \xi'''}^{(3 \rightarrow 1),G',\Lambda'} a_{\xi \rightarrow \xi''}^{(3 \rightarrow 1),G,\Lambda} \right. \\ & \times \int d\Omega^{(1)} B H_{\xi'''}^\dagger(\Omega^{(1)}) V_{23} B H_{\xi''}(\Omega^{(1)}) \\ & + a_{\xi' \rightarrow \xi'''}^{(3 \rightarrow 2),G',\Lambda'} a_{\xi \rightarrow \xi''}^{(3 \rightarrow 2),G,\Lambda} \\ & \left. \left. \times \int d\Omega^{(2)} B H_{\xi'''}^\dagger(\Omega^{(2)}) V_{13} B H_{\xi''}(\Omega^{(2)}) \right] \right\} . \quad (30) \end{aligned}$$

It is then clear the advantage of using the NSHH method also for the calculation of the potential matrix elements, as in fact all what is needed is the calculation of one integral of the type

$$I(\rho) = \int d\Omega^{(p)} B H_{\xi'}^\dagger(\Omega^{(p)}) V_{ij} B H_{\xi''}(\Omega^{(p)}) , \quad (31)$$

with  $p$  the permutation corresponding to the order  $i, j, k$ .

### III. RESULTS

We present in this section the results obtained with the NSHH method described above. In particular, we present in Section III A the study of the convergence of the method, in the case of the triton binding energy, calculated with  $m_p = m_n$ . We then present in Section III B the results for the triton and  $^3\text{He}$  binding energy, when  $m_p \neq m_n$ . In Section III C we present the results of the hypertriton.

The potential models used in our study are central spin-independent and spin-dependent. In particular, the  $^3\text{H}$  and  $^3\text{He}$  systems have been investigated using the spin-independent Volkov [12], Afnan-Tang [13] and Malfliet-Tjon [14] potential models, and the two spin-dependent Minnesota [15] and Argonne AV4' [16] potential models. Note that the AV4' potential is a reprojection of the much more realistic Argonne AV18 [17] potential model. In the case of the hypernucleus  $^3_\Lambda\text{H}$ , we have used the Gaussian spin-independent central potential of Ref. [18], and two spin-dependent potentials: the first one, labeled MN9 [19], combines a Minnesota [15] potential for the  $NN$  interaction with the  $S = 1$  component of the same Minnesota potential multiplied by a factor 0.9 for the  $\Lambda N$  interaction. The second one, labeled AU, uses the Argonne AV4' of Ref. [16] for the  $NN$  interaction, and the Usmani potential of Ref. [20] for the  $\Lambda N$  interaction (see also Ref. [21]).

#### A. Convergence study

We recall that the wave function is written as in Eq. (20), and that, since we are using central potentials, only the first channel of Table I is considered, as for instance in Ref. [1]. Therefore we need to study the convergence of our results on  $G^{max}$  and  $N_{max}$ . Furthermore, we introduce the value of  $j$  as  $\vec{j} = \vec{\ell}_2 + \vec{S}$ ,  $\ell_2$  and  $S$  being the orbital angular momentum and the spin of the pair  $ij$  on which the potential acts. This allows to set up the theoretical framework also in the case of projecting potentials. Therefore, we will study the convergence of our results also on the maximum value of  $j$ , called  $j_{max}$ . Finally, the radial function written as in Eq. (19), presents a non-linear parameter  $\gamma$ , for which

$j_{max} = 6$		$j_{max} = 8$		$j_{max} = 10$	
$G^{max}$	$B$	$G^{max}$	$B$	$G^{max}$	$B$
20	8.460	20	8.462	20	8.462
30	8.461	30	8.464	30	8.464
40	8.461	40	8.464	40	8.465

TABLE II: The  $^3\text{H}$  binding energy  $B$  (in MeV) calculated with the Volkov potential model [12], using  $m_n = m_p$ ,  $N_{max} = 16$  and  $\gamma = 4 \text{ fm}^{-1}$ , as function of  $j_{max}$  and  $G^{max}$ .

$j_{max} = 6$		$j_{max} = 8$		$j_{max} = 10$	
$G^{max}$	$B$	$G^{max}$	$B$	$G^{max}$	$B$
20	8.376	20	8.381	20	8.381
30	8.378	30	8.383	30	8.385
40	8.378	40	8.383	40	8.385

TABLE III: Same as Table II but for the Minnesota potential model [15].

we need to find a range of values such that the binding energy is stable. Note that in these convergence studies we have used  $m_n = m_p$ .

We start by considering the parameter  $\gamma$ . The behaviour of the binding energy as a function of  $\gamma$  is shown for the Volkov potential in the top panel of Fig. 1. We mention here that for all the other potential models we have considered, the results are similar. The other parameters were kept constant, i.e.  $G^{max} = 20$ ,  $N_{max} = 16$  and  $j_{max} = 6$ . The particular dependence on  $\gamma$  of the binding energy, that increases for low values of  $\gamma$ , is constant for some central values, and decreases again for large values of  $\gamma$ , allows to determine a so-called plateau, and the optimal value for  $\gamma$  has to be chosen on this plateau. Alternatively, we can chose  $\gamma$  such that for a given  $N_{max}$  the binding energy is maximum. A choice of  $\gamma$  outside the plateau would require just a larger value of  $N_{max}$ . To be noticed that this particular choice of  $\gamma$  is not universal. As an example, in the “standard” HH method,  $\gamma = 2.5 - 4.5 \text{ fm}^{-1}$  for the AV18 potential, but much larger ( $\simeq 7 \text{ fm}^{-1}$ ) for the chiral non-local potentials [1]. In our case, different values of  $\gamma$  for different potentials might improve the convergence on  $N_{max}$ , but not that on  $j_{max}$  and  $G^{max}$ , determined by the structure of the HH functions. Since, as shown below, the convergence on  $N_{max}$  is not difficult to be achieved, we have chosen to keep  $\gamma$  at a fixed value, i.e.  $\gamma = 4 \text{ fm}^{-1}$  for all the potentials.

In the bottom panel of Fig. 1 we fix  $j_{max} = 8$ ,  $\gamma = 4 \text{ fm}^{-1}$  and  $G^{max} = 20$ , and we show the pattern of convergence for the binding energy  $B$  with respect to  $N_{max}$ , in the case of the Argonne AV4' model. Here convergence is reached for  $N_{max} = 24$ , i.e. we have verified that, for higher  $N_{max}$  value,  $B$  changes by less than 1 keV. To be noticed that for the other potentials, convergence is already reached for  $N_{max} = 16 - 20$ .

The variation of the binding energy as a function of  $j_{max}$  and  $G^{max}$  depends significantly on the adopted potential model. Therefore, we need to analyze every single case. As we can see from the data of Tables II and III, the convergence on  $j_{max}$  and  $G^{max}$  for the Volkov and the Minnesota potentials is really quick, and we can reach an accuracy better than 2 keV for  $j_{max} = 10$  and  $G^{max} = 40$ . On the other hand, in the case of the Afnan-Tang potential, we need to go up to  $j_{max} = 14$  and  $G^{max} = 50$ , in order to get a total accuracy of our results of about 2 keV (1 keV is due to the dependence on  $N_{max}$ ). This can be seen by inspection of Table IV. The Malfliet-Tjon potential model implies a convergence even slower of the expansion, and we have to go up to  $G^{max} = 90$  and  $j_{max} = 22$ , to get an uncertainty of about 3 keV, as shown in Table V. In fact, being a sum of Yukawa functions, the Malfliet-Tjon potential model is quite difficult to be treated also with the “standard” symmetrized HH method [1].

In Tables VI and VII, we show the convergence study for the AV4', which is the most realistic potential model used

$j_{max} = 6$		$j_{max} = 8$		$j_{max} = 10$		$j_{max} = 12$		$j_{max} = 14$	
$G^{max}$	$B$	$G^{max}$	$B$	$G^{max}$	$B$	$G^{max}$	$B$	$G^{max}$	$B$
20	6.567	20	6.617	20	6.619	20	6.619	20	6.619
30	6.605	30	6.664	30	6.682	30	6.688	30	6.688
40	6.608	40	6.668	40	6.687	40	6.693	40	6.695
50	6.608	50	6.668	50	6.687	50	6.694	50	6.696

TABLE IV: Same as Table II but for the Afnan-Tang potential model [13].

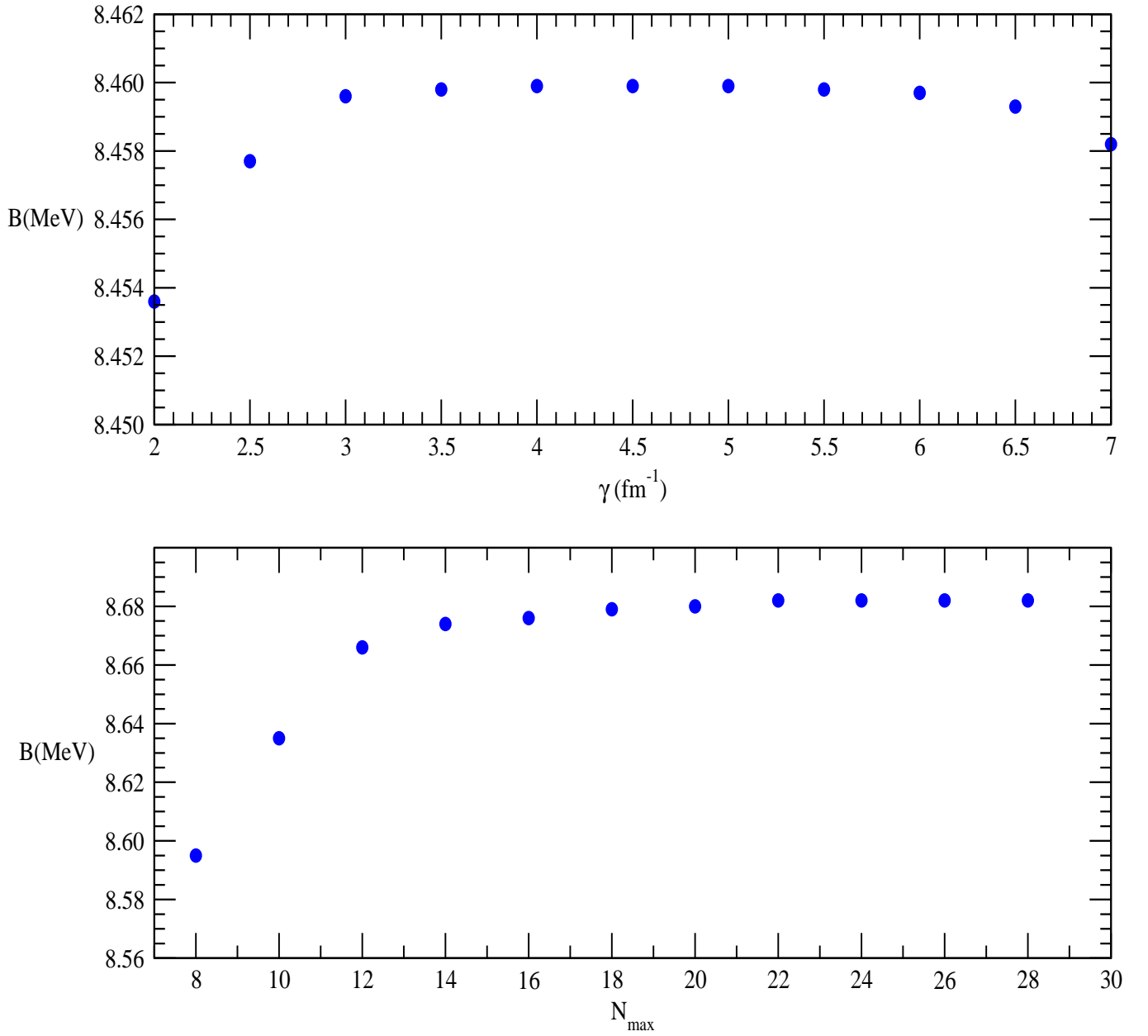


FIG. 1: Top panel: The binding energy  $B$  (in MeV) as function of the parameter  $\gamma$  (in  $\text{fm}^{-1}$ ) for the Volkov potential model [12], with  $G^{\text{max}} = 20$ ,  $j_{\text{max}} = 6$  and  $N_{\text{max}} = 16$ , and using  $m_n = m_p$ . Bottom panel: The binding energy  $B$  (in MeV) as function of the parameter  $N_{\text{max}}$  for the AV4' potential model [16], with  $G^{\text{max}} = 20$ ,  $j_{\text{max}} = 8$  and  $\gamma = 4 \text{ fm}^{-1}$ , and using  $m_n = m_p$ .

here for the  $A = 3$  nuclear systems. As we can see by inspection of the tables, in order to reach an accuracy of about 3 keV, we have to push the calculation up to  $G^{\text{max}} = 80$ ,  $N_{\text{max}} = 24$  and  $j_{\text{max}} = 20$ . Our final result of  $B = 8.991$  MeV, though, agrees well with the one of Ref. [22], obtained with the “standard” symmetrized HH method, for which  $B = 8.992$  MeV.

The results for the binding energy of  $^3\text{H}$  and  $^3\text{He}$  with the different potentials will be summarized in the next Subsection.

$j_{max} = 10$		$j_{max} = 14$		$j_{max} = 18$		$j_{max} = 20$		$j_{max} = 22$	
$G^{max}$	$B$	$G^{max}$	$B$	$G^{max}$	$B$	$G^{max}$	$B$	$G^{max}$	$B$
20	7.943	20	7.943	20	7.943	20	7.943	20	7.943
30	8.155	30	8.179	30	8.179	30	8.179	30	8.179
40	8.182	40	8.222	40	8.229	40	8.229	40	8.229
50	8.190	50	8.231	50	8.241	50	8.243	50	8.243
60	8.192	60	8.234	60	8.244	60	8.246	60	8.247
70	8.193	70	8.235	70	8.245	70	8.248	70	8.249
80	8.194	80	8.235	80	8.246	80	8.248	80	8.249
90	8.194	90	8.235	90	8.246	90	8.248	90	8.250

TABLE V: Same as Table II but for the Malfliet-Tjon potential model [14].

		$j_{max} = 10$		$j_{max} = 12$		$j_{max} = 14$		$j_{max} = 16$	
$N_{max} = 16$	$G^{max}$	$B$	$G^{max}$	$B$	$G^{max}$	$B$	$G^{max}$	$B$	
	20	8.682	20	8.682	20	8.682	20	8.682	
	40	8.923	40	8.956	40	8.970	40	8.975	
	60	8.927	60	8.960	60	8.975	60	8.981	
	80	8.927	80	8.960	80	8.975	80	8.981	
$N_{max} = 20$	$G^{max}$	$B$	$G^{max}$	$B$	$G^{max}$	$B$	$G^{max}$	$B$	
	20	8.686	20	8.686	20	8.686	20	8.686	
	40	8.927	40	8.961	40	8.974	40	8.979	
	60	8.931	60	8.964	60	8.977	60	8.985	
	80	8.931	80	8.964	80	8.977	80	8.985	
$N_{max} = 24$	$G^{max}$	$B$	$G^{max}$	$B$	$G^{max}$	$B$	$G^{max}$	$B$	
	20	8.687	20	8.687	20	8.687	20	8.687	
	40	8.928	40	8.962	40	8.975	40	8.980	
	60	8.932	60	8.965	60	8.980	60	8.986	
	80	8.933	80	8.966	80	8.981	80	8.987	

TABLE VI: The  ${}^3\text{H}$  binding energy  $B$  (in MeV) calculated with the AV4' potential model [16] as function of  $N_{max}$ ,  $j_{max}$  and  $G^{max}$ , using  $m_n = m_p$  and  $\gamma = 4 \text{ fm}^{-1}$ .

### B. The ${}^3\text{H}$ and ${}^3\text{He}$ systems

Having verified that our method can be pushed up to convergence, we present in the third column of Table VIII the results for the  ${}^3\text{H}$  binding energy with all the different potential models, obtained still keeping  $m_p = m_n$ . The results are compared with those present in the literature, finding an overall nice agreement.

We now turn our attention to the  ${}^3\text{H}$  and  ${}^3\text{He}$  nuclei, considering them as made of different mass particles. Therefore, we impose  $m_p \neq m_n$  and we calculate the  ${}^3\text{H}$  and  ${}^3\text{He}$  binding energy and the difference of these binding energies, i.e.

$$\Delta B = B_{{}^3\text{H}} - B_{{}^3\text{He}} . \quad (32)$$

To be noticed that we have not yet included the effect of the (point) Coulomb interaction. The results are listed in Table VIII. By inspection of the table, we can see that  $\Delta B$  is not the same for all the potential models. In fact, while for the spin-independent Afnan-Tang and Malfliet-Tjon central potentials, and for the spin-dependent AV4' potential,  $\Delta B = 14 \text{ keV}$ , for the Volkov and the Minnesota potential we find a smaller value. In all cases, though, we have

$j_{max}$	10	12	14	16	18	20
$B$	8.932	8.965	8.980	8.986	8.989	8.991

TABLE VII: The  ${}^3\text{H}$  binding energy  $B$  (in MeV) calculated with the AV4' potential model [16], using  $m_n = m_p$ ,  $G^{max} = 60$ ,  $N_{max} = 24$  and  $\gamma = 4 \text{ fm}^{-1}$ .



Potential model	literature	$B(m_p = m_n)$	$B_{^3\text{H}}$	$B_{^3\text{He}}$	$\Delta B$	$BC_{^3\text{He}}$
Volkov	8.465 [1]	8.465	8.470	8.459	0.011	7.754
Afnan-Tang	6.698 [22]	6.697	6.704	6.690	0.014	5.990
Malfliet-Tjon	8.253 [1]	8.250	8.257	8.243	0.014	7.516
Minnesota	8.386 [1]	8.385	8.389	8.381	0.008	7.706
AV4'	8.992 [22]	8.991	8.998	8.984	0.014	8.272

TABLE VIII: The  $^3\text{H}$  binding energy obtained using  $m_n = m_p$  ( $B(m_p = m_n)$ ), the  $^3\text{H}$  and  $^3\text{He}$  binding energies calculated taking into account the difference of masses but no Coulomb interaction in  $^3\text{He}$  ( $B_{^3\text{H}}$  and  $B_{^3\text{He}}$ ), the difference  $\Delta B = B_{^3\text{H}} - B_{^3\text{He}}$ , and the  $^3\text{He}$  binding energy calculated including also the (point) Coulomb interaction ( $BC_{^3\text{He}}$ ). All the values are given in MeV. The results present in the literature for  $B(m_p = m_n)$  are also listed with the corresponding references.

verified that  $\Delta B$  is equally distributed, i.e. we have verified that

$$B_{m_n=m_p} = B_{^3\text{H}} - \frac{\Delta B}{2} = B_{^3\text{He}} + \frac{\Delta B}{2}, \quad (33)$$

as can be seen from Table VIII. We would like to remark that in the NSHH method, the inclusion of the difference of masses is quite straightforward, and  $\Delta B$  can be calculated “exactly”. This is not so trivial within the symmetrized HH method. Furthermore, we compare our results with those of Ref. [23], where  $\Delta B$  was calculated within the Faddeev equation method using realistic Argonne AV18 [17] potential, and it was found  $\Delta B = 14$  keV, in perfect agreement with our AV4' result.

In order to test our results for  $\Delta B$ , we try to get a perturbative rough estimate of  $\Delta B$ , proceeding as follows: since the neutron-proton difference of mass  $\Delta m = m_n - m_p = 1.2934$  MeV is about three orders of magnitude smaller than their average mass  $m = (m_n + m_p)/2 = 938.9187$  MeV, we can assume also  $\Delta B$  to be small. Furthermore, we suppose the potential to be insensitive to  $\Delta m$ , and we consider only the kinetic energy. In the center of mass frame, the kinetic energy operator can be cast in the form

$$T = \sum_{i=1}^3 \frac{\mathbf{p}_i^2}{2m_i} = \frac{\mathbf{p}_1^2 + \mathbf{p}_2^2}{2m_e} + \frac{\mathbf{p}_3^2}{2m_d}, \quad (34)$$

where  $m_e$  stands for the mass of the two equal particles, i.e.  $m_n$  for  $^3\text{H}$  and  $m_p$  for  $^3\text{He}$ , and  $m_d$  is the mass of the third particle, different from the previous ones. By defining  $E = \langle H \rangle = \langle T + V \rangle$ , where  $\langle H \rangle$  is the average value of the Hamiltonian  $H$ , we obtain

$$\frac{\partial E}{\partial m_e} = \left\langle \frac{\partial H}{\partial m_e} \right\rangle = \left\langle \frac{\partial T}{\partial m_e} \right\rangle = -\frac{\langle 2T_e \rangle}{m_e}, \quad (35)$$

$$\frac{\partial E}{\partial m_d} = \left\langle \frac{\partial H}{\partial m_d} \right\rangle = \left\langle \frac{\partial T}{\partial m_d} \right\rangle = -\frac{\langle T_d \rangle}{m_d}, \quad (36)$$

where we have indicated  $\langle T_{e/d} \rangle \approx \mathbf{p}_i^2/(2m_{e/d})$ . Moreover, we define the proton and neutron mass difference  $\Delta m_{p/n}$  as

$$\Delta m_p \equiv m_p - m = -\frac{\Delta m}{2}, \quad (37)$$

$$\Delta m_n \equiv m_n - m = \frac{\Delta m}{2}, \quad (38)$$

and the  $^3\text{He}$  and  $^3\text{H}$  binding energy difference  $\Delta B_{^3\text{He}/^3\text{H}}$  as

$$\Delta B_{^3\text{He}} \equiv B_{m_n=m_p} - B_{^3\text{He}}, \quad (39)$$

$$\Delta B_{^3\text{H}} \equiv B_{m_n=m_p} - B_{^3\text{H}}. \quad (40)$$

Potential model	$\langle T \rangle$ (MeV)	$\Delta B_{PT}$ (MeV)	$\Delta B_{NSHH}$ (MeV)
Volkov	23.798	0.011	0.011
Afnan-Tang	30.410	0.014	0.014
Malfliet-Tjon	30.973	0.014	0.014
Minnesota	27.216	0.012	0.008
AV4'	37.599	0.017	0.014

TABLE IX: Mean value for the kinetic energy operator  $\langle T \rangle$ ,  $\Delta B$  estimated with the perturbative theory ( $PT$ ), and  $\Delta B$  calculated with the NSHH for the different potential models considered in this work. See text for more details.

Then using Eqs. (35)–(38), we obtain

$$\begin{aligned} \Delta B_{^3\text{He}} &\approx \frac{\partial E}{\partial m_e} \Delta m_p + \frac{\partial E}{\partial m_d} \Delta m_n = \frac{\langle 2T_e \rangle}{m_e} \frac{\Delta m}{2} - \frac{\langle T_d \rangle}{m_d} \frac{\Delta m}{2} \\ &\approx \langle 2T_e - T_d \rangle \frac{\Delta m}{2m}. \end{aligned} \quad (41)$$

$$\begin{aligned} \Delta B_{^3\text{H}} &\approx \frac{\partial E}{\partial m_e} \Delta m_n + \frac{\partial E}{\partial m_d} \Delta m_p = -\frac{\langle 2T_e \rangle}{m_e} \frac{\Delta m}{2} + \frac{\langle T_d \rangle}{m_d} \frac{\Delta m}{2} \\ &\approx -\langle 2T_e - T_d \rangle \frac{\Delta m}{2m}. \end{aligned} \quad (42)$$

In conclusion

$$\Delta B_{PT} \equiv B_{^3\text{H}} - B_{^3\text{He}} \approx \langle 2T_e - T_d \rangle \frac{\Delta m}{m} \approx \langle T \rangle \frac{\Delta m}{3m}, \quad (43)$$

where the last equality holds assuming that  $\langle T_e \rangle = \langle T_d \rangle = \langle T \rangle / 3$ , since the  $^3\text{He}$  and  $^3\text{H}$  have a large  $S$ -wave component (about 90 %). The results of  $\langle T \rangle$  and  $\Delta B_{PT}$  are listed in Table IX, and are compared with the values for  $\Delta B$  calculated within the NSHH and already listed in Table VIII. By inspection of the table we can see an overall nice agreement between this rough estimate and the exact calculation for all the potential models. Only in the case of the Minnesota and AV4' potentials,  $\Delta B_{PT}$  is 4 and 3 keV larger than  $\Delta B$ , respectively. This can be understood by noticing that these potentials are spin-dependent, giving rise to mixed-symmetry components in the wave functions. These components are responsible for a reduction in  $\Delta B_{PT}$  [24], related to the fact that the nuclear force for the  $^3\text{S}_1$   $np$  pair is stronger than for the  $^1\text{S}_0$   $nn$  (or  $pp$ ) pair. Therefore, the kinetic energy for equal particles  $\langle T_e \rangle$  is less than the kinetic energy for different particles  $\langle T_d \rangle$ .

### C. The $^3_\Lambda\text{H}$ hypernucleus

The hypernucleus  $^3_\Lambda\text{H}$  is a bound system composed by a neutron, a proton and the  $\Lambda$  hyperon. In order to study this system, we have considered the proton and the neutron as reference-pair, with equal mass  $m_n = m_p = m$ , while the  $\Lambda$  particle has been taken as the third particle with different mass. The  $\Lambda$  hyperon mass has been chosen depending on the considered potential. We remind that we have used three different potential models: a central spin-independent Gaussian model [18], and two spin-dependent central potentials, labelled MN9 [19] and AU [21] potentials. Therefore, when the  $^3_\Lambda\text{H}$  hypernucleus has been studied using the Gaussian potential of Ref. [18], we have set  $M_\Lambda = 6/5 m_N$ , accordingly. In the other two cases, we have used  $M_\Lambda = 1115.683$  MeV. We first study the convergence pattern of our method, which in the case of the Gaussian potential of Ref. [18] is really fast, with a reached accuracy of 1 keV on the binding energy already with  $N_{max} = 20$ ,  $j_{max} = 10$  and  $G^{max} = 50$ . This can be seen directly by inspection of Tables X and XI.

The convergence pattern in the case of the spin-dependent central MN9 and AU potentials has been found quite slower. This is shown in Tables XII and XIII, respectively. By inspection of Table XII, we can conclude that  $B = 2.280$  MeV, with an accuracy of about 3 keV, obtained with  $G^{max} = 100$ ,  $N_{max} = 34$ , and  $j_{max} = 14$ . By inspection of Table XIII,  $B = 2.532$  MeV, with an accuracy of about 4 keV, going up to  $G^{max} = 140$ ,  $N_{max} = 24$  and  $j_{max} = 16$ .

The results obtained with our method for the three potential models considered in this work are compared with those present in the literature [18, 19, 21] in Table XIV, finding a very nice agreement, within the reached accuracy.

$j_{max} = 6$		$j_{max} = 8$		$j_{max} = 10$	
$G^{max}$	$B$	$G^{max}$	$B$	$G^{max}$	$B$
0	0.510	0	0.510	0	0.510
2	1.070	2	1.070	2	1.070
4	1.776	4	1.776	4	1.776
6	2.211	6	2.211	6	2.211
8	2.371	8	2.371	8	2.371
10	2.476	10	2.476	10	2.476
12	2.551	12	2.551	12	2.551
20	2.659	20	2.660	20	2.660
30	2.692	30	2.693	30	2.693
40	2.700	40	2.701	40	2.701
50	2.702	50	2.703	50	2.703

TABLE X: The  ${}^3_{\Lambda}\text{H}$  binding energy  $B$  (in MeV) as function of  $j_{max}$  and  $G^{max}$ , calculated with the Gaussian potential model of Ref. [18], using  $N_{max} = 20$  and  $\gamma = 4 \text{ fm}^{-1}$ .

$N_{max}$	8	12	16	20
$B$	2.552	2.651	2.660	2.660

TABLE XI: The  ${}^3_{\Lambda}\text{H}$  binding energy  $B$  (in MeV) as function of  $N_{max}$ , calculated with the the Gaussian potential model of Ref. [18], using  $G^{max} = 20$ ,  $j_{max} = 8$  and  $\gamma = 4 \text{ fm}^{-1}$ .

#### IV. CONCLUSIONS AND OUTLOOK

In this work we present a study of the bound state of a three-body system, composed of different particles, by means of the NSHH method. The method has been reviewed in Section II. In order to verify its validity, we have started by considering a system of three equal-mass nucleons interacting via different central potential models, three spin-independent and two spin-dependent. We have studied the convergence pattern, and we have compared our results at convergence with those present in the literature, finding an overall nice agreement. Then, we have switched on the difference of mass between protons and neutrons and we have calculated the difference of binding energy  $\Delta B$  due to the difference between the neutron and proton masses. We have found that  $\Delta B$  depends on the considered potential model, but is always symmetrically distributed (see Eq. (33)).

Finally we have implemented our method for the  ${}^3_{\Lambda}\text{H}$  hypernucleus, studied with three different potentials, i.e. the Gaussian potential of Ref. [18], for which we have found a fast convergence of the NSHH method, the MN9 and the AU potentials of Ref. [19], for which the convergence is much slower. In these last two cases, in particular, we had found necessary to include a large number of the HH basis (46104 for the MN9 and 52704 for the AU potentials), but the agreement with the results in the literature has been found quite nice. To be noticed that we have included only two-body interactions, and therefore a comparison with the experimental data is meaningless.

In conclusion, we believe that we have proven the NSHH method to be a good choice for studying three-body systems composed of two equal mass particles, different from the mass of the third particle. Besides  ${}^3\text{H}$ ,  ${}^3\text{He}$ , and  ${}^3_{\Lambda}\text{H}$ , several other nuclear systems can be viewed as three-body systems of different masses. This applies in all cases where a strong clusterization is present, as in the case of  ${}^6\text{He}$  and  ${}^6\text{Li}$  nuclei, seen as  $NN\alpha$ , or the  ${}^9\text{Be}$  and  ${}^9\text{B}$ , seen as  $\alpha\alpha N$  three-body systems. Furthermore, taking advantage of the versatility of the HH method also for scattering systems, the NSHH approach could be extended as well to scattering problems. Work along these lines are currently underway.

#### Acknowledgments

The authors would like to thank Dr. F. Ferrari Ruffino for useful discussions. Computational resources provided by the INFN-Pisa Computer Center are gratefully acknowledged.

## V. APPENDIX: THE TRANSFORMATION COEFFICIENTS

Let us start by writing Eq. (29) as

$$a_{\ell_1, \ell_2, n, \ell'_1, \ell'_2, n'}^{(p \rightarrow p'), G, \Lambda} = \int d\Omega^{(p')} [H_{[\ell'_1, \ell'_2, n', \Lambda \Lambda_z]}(\Omega^{(p')})]^\dagger H_{[\ell_1, \ell_2, n, \Lambda \Lambda_z]}(\Omega^{(p)}) , \quad (44)$$

where  $\ell_i$  ( $\ell'_i$ ) is the orbital angular momentum associated with the Jacobi coordinate  $\mathbf{y}_i^{(p)}$  ( $\mathbf{y}_i^{(p')}$ ). It can be demonstrated by direct calculation and exploiting the spherical harmonics proprieties that

$$\begin{aligned} a_{\ell_1, \ell_2, n, \ell'_1, \ell'_2, n'}^{(p \rightarrow p'), G, L} &= N_{n'}^{\ell'_1, \ell'_2} N_n^{\ell_1, \ell_2} \frac{1}{2} \int_0^{\frac{\pi}{2}} d\phi \int_{-1}^1 d\mu (\cos \phi^{(p')})^{2+\ell'_2} (\sin \phi^{(p')})^{2+\ell'_1} \\ &\times P_{n'}^{\ell'_1+1/2, \ell'_2+1/2}(\cos 2\phi^{(p')}) P_n^{\ell_1+1/2, \ell_2+1/2}(\cos 2\phi^{(p)}) \\ &\times \sum_{\lambda, \lambda_1, \lambda_2} C_{\ell_1, \ell_2, \lambda_1, \lambda_2}^{(p), (p')}(\sin \phi^{(p')}, \cos \phi^{(p')}) P_\lambda(\mu) \\ &\times (-)^{\Lambda+\lambda_2+\ell'_2} (2\lambda+1) \hat{\ell}'_1 \hat{\ell}'_2 \hat{\lambda}_1 \hat{\lambda}_2 \\ &\times \begin{Bmatrix} \ell'_1 & \ell'_2 & \Lambda \\ \lambda_2 & \lambda_1 & \lambda \end{Bmatrix} \begin{pmatrix} \ell'_1 & \lambda_1 & \lambda \\ 0 & 0 & 0 \end{pmatrix} \begin{pmatrix} \ell'_2 & \lambda_2 & \lambda \\ 0 & 0 & 0 \end{pmatrix} . \end{aligned} \quad (45)$$

Here the curly brackets indicate the  $6j$  Wigner coefficients, and the coefficients  $C_{\ell_1, \ell_2, \ell'_1, \ell'_2}^{(p), (p')}(\sin \phi^{(p')}, \cos \phi^{(p')})$  are defined as

$$\begin{aligned} C_{\ell_1, \ell_2, \ell'_1, \ell'_2}^{(p), (p')}(\sin \phi^{(p')}, \cos \phi^{(p')}) &= \sum_{\lambda_1+\lambda_2=\ell_1} \sum_{\lambda'_1+\lambda'_2=\ell_2} (\sin \phi^{(p')})^{\lambda_1+\lambda'_1} (\cos \phi^{(p')})^{\lambda_2+\lambda'_2} \\ &\times (\alpha_{11(p')}^{(p)})^{\lambda_1} (\alpha_{12(p')}^{(p)})^{\lambda_2} (\alpha_{21(p')}^{(p)})^{\lambda'_1} (\alpha_{22(p')}^{(p)})^{\lambda'_2} \\ &\times (-)^{\lambda_1+\lambda_2+\lambda'_1+\lambda'_2} D_{\ell_1, \lambda_1, \lambda_2} D_{\ell_2, \lambda'_1, \lambda'_2} \\ &\times \hat{\ell}_1 \hat{\ell}_2 \hat{\ell}'_1 \hat{\ell}'_2 \hat{\lambda}_1 \hat{\lambda}_2 \hat{\lambda}'_1 \hat{\lambda}'_2 \begin{pmatrix} \lambda_1 & \lambda'_1 & \ell'_1 \\ 0 & 0 & 0 \end{pmatrix} \\ &\times \begin{pmatrix} \lambda_2 & \lambda'_2 & \ell'_2 \\ 0 & 0 & 0 \end{pmatrix} \begin{Bmatrix} \lambda_1 & \lambda_2 & \ell_1 \\ \lambda'_1 & \lambda'_2 & \ell_2 \\ \ell'_1 & \ell'_2 & \Lambda \end{Bmatrix} . \end{aligned} \quad (46)$$

In Eq. (46)  $\hat{\ell} \equiv \sqrt{2\ell+1}$ , and the round (curly) brackets denote  $3j$  ( $9j$ ) Wigner coefficients. The coefficients  $\alpha_{ij(p')}^{(p)}$ , with  $ij = 1, 2$  are given by

$$\mathbf{y}_i^{(p)} = \sum_{j=1}^2 \alpha_{ij(p')}^{(p)} \mathbf{y}_j^{(p')} , \quad (47)$$

and depend on the (different) masses of the three particles. and  $D_{\ell, \ell_a, \ell_b}$  is defined as

$$D_{\ell, \ell_a, \ell_b} = \sqrt{\frac{(2\ell+1)!}{(2\ell_a+1)!(2\ell_b+1)!}} . \quad (48)$$

- 
- [1] A. Kievsky, S. Rosati, M. Viviani, L. E. Marcucci, and L. Girlanda, J. Phys. G **35**, 063101 (2008), 0805.4688.
  - [2] W. Leidemann and G. Orlandini, Prog. Part. Nucl. Phys. **68**, 158 (2013), 1204.4617.
  - [3] M. Gattobigio, A. Kievsky, M. Viviani, and P. Barletta, Phys. Rev. **A79**, 032513 (2009), 0811.4259.
  - [4] M. Gattobigio, A. Kievsky, M. Viviani, and P. Barletta, Few-Body Syst. **45**, 127 (2009), ISSN 1432-5411, URL <https://doi.org/10.1007/s00601-009-0045-4>.
  - [5] M. Gattobigio, A. Kievsky, and M. Viviani, Phys. Rev. **C83**, 024001 (2011), 1009.3426.

- [6] S. Deflorian, N. Barnea, W. Leidemann, and G. Orlandini, *Few-Body Syst.* **54**, 1879 (2013), 1212.5532.
- [7] S. Deflorian, N. Barnea, W. Leidemann, and G. Orlandini, *Few-Body Syst.* **55**, 831 (2014).
- [8] S. Rosati, in *Introduction to Modern Methods of Quantum Many-Body Theory and Their Applications, Series on Advances in Quantum Many-Body Theory, vol. 7*, edited by A. Fabrocini, S. Fantoni, and E. Krotscheck (World Scientific, 2002), p. 339.
- [9] C. R. Chen, G. L. Payne, J. L. Friar, and B. F. Gibson, *Phys. Rev. C* **33**, 1740 (1986), URL <https://link.aps.org/doi/10.1103/PhysRevC.33.1740>.
- [10] A. Edmonds, *Angular Momentum in Quantum Mechanics* (Princeton University Press, Princeton, New Jersey, 1974).
- [11] J. Raynal and J. Revai, *Il Nuovo Cimento A* (1965-1970) **68**, 612 (1970), ISSN 1826-9869, URL <https://doi.org/10.1007/BF02756127>.
- [12] A. Volkov, *Nucl. Phys.* **74**, 33 (1965), ISSN 0029-5582, URL <http://www.sciencedirect.com/science/article/pii/0029558265902440>.
- [13] I. R. Afnan and Y. C. Tang, *Phys. Rev.* **175**, 1337 (1968), URL <https://link.aps.org/doi/10.1103/PhysRev.175.1337>.
- [14] R. Malfliet and J. Tjon, *Phys. Lett. B* **30**, 293 (1969), ISSN 0370-2693, URL <http://www.sciencedirect.com/science/article/pii/0370269369904833>.
- [15] D. Thompson, M. Lemere, and Y. Tang, *Nucl. Phys. A* **286**, 53 (1977), ISSN 0375-9474, URL <http://www.sciencedirect.com/science/article/pii/0375947477900070>.
- [16] R. B. Wiringa and S. C. Pieper, *Phys. Rev. Lett.* **89**, 182501 (2002), URL <https://link.aps.org/doi/10.1103/PhysRevLett.89.182501>.
- [17] R. B. Wiringa, V. G. J. Stoks, and R. Schiavilla, *Phys. Rev. C* **51**, 38 (1995), URL <https://link.aps.org/doi/10.1103/PhysRevC.51.38>.
- [18] R. B. Clare and J. S. Levinger, *Phys. Rev. C* **31**, 2303 (1985), URL <https://link.aps.org/doi/10.1103/PhysRevC.31.2303>.
- [19] F. Ferrari Ruffino, *Non-Symmetrized Hyperspherical Harmonics Method Applied to Light Hypernuclei* (PhD Thesis, University of Trento, Trento (Italy), 2017).
- [20] A. A. Usmani and F. C. Khanna, *J. Phys. G* **35**, 025105 (2008), URL <http://stacks.iop.org/0954-3899/35/i=2/a=025105>.
- [21] F. Ferrari Ruffino, N. Barnea, S. Deflorian, W. Leidemann, D. Lonardoni, G. Orlandini, and F. Pederiva, *Few-Body Syst.* **58**, 113 (2017).
- [22] L. Marcucci (2018).
- [23] A. Nogga, A. Kievsky, H. Kamada, W. Glöckle, L. E. Marcucci, S. Rosati, and M. Viviani, *Phys. Rev. C* **67**, 034004 (2003), URL <https://link.aps.org/doi/10.1103/PhysRevC.67.034004>.
- [24] J. L. Friar, B. F. Gibson, and G. L. Payne, *Phys. Rev. C* **42**, 1211 (1990).

$j_{max} = 6$		$j_{max} = 10$		$j_{max} = 12$		$j_{max} = 14$		
$N_{max} = 16$	$G^{max}$	$B$	$G^{max}$	$B$	$G^{max}$	$B$	$G^{max}$	$B$
	50	2.174	50	2.201	50	2.205	50	2.207
	60	2.178	60	2.205	60	2.209	60	2.211
	70	2.181	70	2.207	70	2.211	70	2.213
	80	2.181	80	2.208	80	2.212	80	2.214
	90	2.182	90	2.208	90	2.212	90	2.215
	100	2.182	100	2.208	100	2.212	100	2.215
$N_{max} = 20$	$G^{max}$	$B$	$G^{max}$	$B$	$G^{max}$	$B$	$G^{max}$	$B$
	50	2.206	50	2.232	50	2.236	50	2.239
	60	2.213	60	2.238	60	2.242	60	2.245
	70	2.216	70	2.241	70	2.246	70	2.248
	80	2.219	80	2.243	80	2.248	80	2.250
	90	2.220	90	2.244	90	2.249	90	2.251
	100	2.220	100	2.244	100	2.249	100	2.252
$N_{max} = 24$	$G^{max}$	$B$	$G^{max}$	$B$	$G^{max}$	$B$	$G^{max}$	$B$
	50	2.219	50	2.243	50	2.247	50	2.250
	60	2.227	60	2.251	60	2.255	60	2.257
	70	2.232	70	2.255	70	2.259	70	2.261
	80	2.235	80	2.257	80	2.261	80	2.264
	90	2.236	90	2.259	90	2.263	90	2.266
	100	2.236	100	2.260	100	2.264	100	2.267
$N_{max} = 28$	$G^{max}$	$B$	$G^{max}$	$B$	$G^{max}$	$B$	$G^{max}$	$B$
	50	2.222	50	2.248	50	2.252	50	2.255
	60	2.233	60	2.257	60	2.261	60	2.264
	70	2.240	70	2.263	70	2.267	70	2.269
	80	2.244	80	2.266	80	2.270	80	2.272
	90	2.246	90	2.268	90	2.272	90	2.274
	100	2.248	100	2.269	100	2.273	100	2.276
$N_{max} = 32$	$G^{max}$	$B$	$G^{max}$	$B$	$G^{max}$	$B$	$G^{max}$	$B$
	50	2.225	50	2.249	50	2.253	50	2.256
	60	2.236	60	2.258	60	2.262	60	2.265
	70	2.243	70	2.264	70	2.268	70	2.272
	80	2.247	80	2.268	80	2.273	80	2.275
	90	2.250	90	2.272	90	2.275	90	2.277
	100	2.252	100	2.273	100	2.276	100	2.279
$N_{max} = 34$	$G^{max}$	$B$	$G^{max}$	$B$	$G^{max}$	$B$	$G^{max}$	$B$
	50	2.225	50	2.249	50	2.253	50	2.256
	60	2.237	60	2.259	60	2.263	60	2.266
	70	2.244	70	2.265	70	2.269	70	2.272
	80	2.248	80	2.269	80	2.274	80	2.276
	90	2.251	90	2.273	90	2.276	90	2.278
	100	2.253	100	2.274	100	2.277	100	2.280

TABLE XII: The  ${}^3_\Lambda\text{H}$  binding energy  $B$  (in MeV) as function of  $G^{max}$ ,  $j_{max}$  and  $N_{max}$ , calculated with the MN9 potential model of Ref. [19], using  $\gamma = 4 \text{ fm}^{-1}$ .

$j_{max} = 6$		$j_{max} = 10$		$j_{max} = 12$		$j_{max} = 14$		$j_{max} = 16$		
$N_{max} = 16$	$G^{max}$	$B$	$G^{max}$	$B$	$G^{max}$	$B$	$G^{max}$	$B$	$G^{max}$	$B$
	20	1.436	20	1.508	20	1.521	20	1.521	20	1.521
	30	1.924	30	2.037	30	2.051	30	2.056	30	2.056
	40	2.137	40	2.243	40	2.258	40	2.267	40	2.270
	50	2.250	50	2.349	50	2.363	50	2.372	50	2.375
	60	2.314	60	2.408	60	2.421	60	2.430	60	2.433
	70	2.355	70	2.445	70	2.455	70	2.461	70	2.467
	80	2.379	80	2.466	80	2.476	80	2.484	80	2.485
	90	2.394	90	2.479	90	2.489	90	2.497	90	2.499
	100	2.402	100	2.486	100	2.498	100	2.503	100	2.506
	110	2.406	110	2.489	110	2.504	110	2.510	110	2.514
	120	2.408	120	2.491	120	2.507	120	2.513	120	2.518
	130	2.409	130	2.492	130	2.509	130	2.515	130	2.520
	140	2.409	140	2.492	140	2.510	140	2.516	140	2.521
$N_{max} = 20$	$G^{max}$	$B$	$G^{max}$	$B$	$G^{max}$	$B$	$G^{max}$	$B$	$G^{max}$	$B$
	20	1.438	20	1.522	20	1.522	20	1.522	20	1.522
	30	1.925	30	2.038	30	2.053	30	2.057	30	2.057
	40	2.139	40	2.245	40	2.259	40	2.268	40	2.271
	50	2.252	50	2.351	50	2.364	50	2.373	50	2.376
	60	2.317	60	2.409	60	2.423	60	2.431	60	2.435
	70	2.357	70	2.446	70	2.458	70	2.466	70	2.469
	80	2.384	80	2.470	80	2.480	80	2.488	80	2.491
	90	2.402	90	2.485	90	2.495	90	2.501	90	2.505
	100	2.413	100	2.494	100	2.504	100	2.512	100	2.515
	110	2.421	110	2.501	110	2.510	110	2.518	110	2.521
	120	2.426	120	2.505	120	2.514	120	2.521	120	2.525
	130	2.429	130	2.507	130	2.516	130	2.524	130	2.527
	140	2.430	140	2.508	140	2.517	140	2.526	140	2.528
$N_{max} = 24$	$G^{max}$	$B$	$G^{max}$	$B$	$G^{max}$	$B$	$G^{max}$	$B$	$G^{max}$	$B$
	20	1.438	20	1.523	20	1.523	20	1.524	20	1.524
	30	1.926	30	2.039	30	2.053	30	2.057	30	2.057
	40	2.139	40	2.245	40	2.259	40	2.268	40	2.271
	50	2.252	50	2.351	50	2.364	50	2.373	50	2.377
	60	2.317	60	2.410	60	2.423	60	2.432	60	2.435
	70	2.357	70	2.446	70	2.458	70	2.467	70	2.470
	80	2.385	80	2.471	80	2.481	80	2.488	80	2.492
	90	2.402	90	2.485	90	2.496	90	2.502	90	2.506
	100	2.414	100	2.494	100	2.505	100	2.513	100	2.516
	110	2.423	110	2.502	110	2.511	110	2.519	110	2.522
	120	2.429	120	2.507	120	2.516	120	2.523	120	2.526
	130	2.433	130	2.510	130	2.519	130	2.527	130	2.530
	140	2.437	140	2.511	140	2.521	140	2.530	140	2.532

TABLE XIII: Same as Table XII but using the AU potential model of Ref. [21] for  $N_{max} = 16, 20, 24$ .

Potential model	$B$	literature
Gaussian	2.703	2.71 [18]
MN9	2.280	2.27 [19]
AU	2.532	2.530 [21]

TABLE XIV: The  ${}^3_\Lambda\text{H}$  binding energy  $B$  (in MeV) obtained in the present work is compared with the results present in the literature.